

THE CORROSION OF REFRACTORIES IN CONTACT WITH SILICEOUS MINERAL RESIDUES AT HIGH TEMPERATURES

C. R. Kennedy

Materials Science Division, Argonne National Laboratory,
Argonne, Illinois 60439, USA

Abstract - The compatibility of a variety of refractories with three different siliceous mineral residues at temperatures between 1500 and 1600°C has been investigated, and the corrosion mechanisms have been identified. Dense high-chromia refractories were found to demonstrate excellent resistance to corrosion. The superiority of chromia-based refractories relative to alumina-based refractories increased as the CaO/SiO₂ ratio and alumina content of the residue increased and decreased, respectively. Water cooling significantly reduced the corrosion of many of the refractories tested.

INTRODUCTION

The corrosion of refractories by molten mineral residues (MRs) at high temperatures is of concern in many industrial processes. This paper details the results of three tests that have been conducted to evaluate the compatibility of a variety of refractories with three MRs at high temperatures in a low-oxygen atmosphere ($p_{O_2} \sim 10^{-3}$ to 10^{-5} Pa). The chemical compositions of the refractories and MRs are given in Tables 1 and 2, respectively (information on the origins of the MRs is proprietary). These tests provide a relative ranking of the corrosion resistances of the refractories. The results from these tests should not be used to predict actual refractory lifetimes in any particular application.

EXPERIMENTAL PROCEDURE

In Fig. 1, a schematic diagram of the test furnace is shown. The furnace was fired by natural gas, oxygen, and air. A reducing atmosphere was maintained by utilizing excess natural gas. The furnace temperature was measured with a Pt vs Pt-10% Rh thermocouple.

The refractory samples were arranged around the circumference of the furnace shell to form a ring, into which was charged up to 80 kg of MR. Some rotary motion of this bath was induced by the flames from the three burners, since the burners were oriented in such a manner as to fire tangentially to the circumference of the MR bath. The MR was sampled regularly and wet chemical analysis was performed on these samples.

After termination of the test, the bricks were removed from the furnace and sectioned lengthwise in the vertical plane so that the MR attack (depth of material removed and depth of MR penetration) could be viewed in cross section.

Metallographic and scanning electron microscopic examination of selected samples were utilized to determine the corrosion mechanisms.

RESULTS

Test 2400B

This test evaluated the compatibility of 11 different brands of refractory bricks (~228 mm in length) with a very acidic (CaO/SiO₂ = 0.15) high-iron oxide MR (Table 2).

In the initial phase of the test, designated 2400B-1, the refractories were exposed to an MR bath about 45 mm deep (40 kg of MR) at a plenum temperature of 1600°C for a total of 250 h. The furnace was then cooled to room temperature to allow visual observation of the corrosion. For test run 2400B-2, an additional ~40 kg of MR was then added (to bring the MR bath to 90 mm in depth) and the furnace was heated to 1500°C for 500 h. During both phases of this test, a reducing atmosphere was maintained.

TABLE 1. Characteristics of test refractories (data provided by manufacturer)

Number	Primary Phase(s)	Bond	Average Apparent Porosity (%)	Composition (wt %)									
				Cr ₂ O ₃	Al ₂ O ₃	Fe ₂ O ₃	MgO	ZrO ₂	SiO ₂	CaO	TiO ₂		
100	Alumina	Alumina-Chromia SS ^a	8	10.0	90.0	NA ^b	-	-	NA	NA	NA		
16	↓	↓	18	10.0	89.7	0.1	-	-	~0.1	-	-		
16I			17	10.0	89.7	0.1	-	-	~0.1	-	-		
852M			13	9.8	87.9	0.5	-	-	0.5	-	-		
852			13	16.6	81.1	0.5	-	-	0.5	-	-		
23			17	10.0	89.7	0.1	-	-	0.1	-	-		
23A			19	15.0	85.0	0.1	0.5	-	0.5	0.3	-		
23B			20	20.0	80.0	0.1	0.5	-	0.5	0.3	-		
38			Alumina-Chromia SS, Spinel	Direct	4	27.3	60.4	4.2	6.0	-	1.8	-	-
22			Spinel, Chromia	Direct	6	79.7	4.7	6.1	8.1	-	1.3	-	-
280			Alumina-Chromia SS	Direct	3	32.0	65.0	1.2	0.6	-	0.2	0.6	-
255	Spinel, Chromia	Si-Ti-rich Glass	2-10	79.0	6.0	5.0	5.0	-	3.0	0.2	1.6		
412	Spinel, Magnesia	Direct	16	43.0	9.0	12.5	33.5	-	1.3	0.5	-		
812	Spinel, Chromia	Direct	9	78.0	1.0	1.5	18.0	-	0.5	0.5	-		
600	Chromia-Alumina SS	Si-rich Glass	12	60.0	20.0	0.1	0.1	12.0	6.5	0.1	0.7		
300	Alumina-Chromia SS	Si-rich Glass	9	31.5	40.8	0.1	0.1	17.0	9.0	0.1	0.5		
251A	Spinel, Magnesia (Minor)	Direct	17	72.8	0.4	0.6	25.5	-	0.6	-	0.1		
251B	Spinel, Magnesia (Minor)	Direct	16	63.2	3.4	5.7	26.2	-	1.3	-	0.2		
800	Chromia	Si-Al-rich Glass	13	76.0	9.0	-	-	-	10.5	NA	3.0		

^aSS = solid solution.
^bNA = not available.

TABLE 2. Average composition (wt %),^a CaO/SiO₂ ratio, and ferritic content (%)^b of the mineral residues

	MR 2400B	MR 2400A	MR 2400C
SiO ₂	42.4	47.3	51.4
CaO	6.5	6.6	21.7
Al ₂ O ₃	22.8	23.6	14.6
FeO	19.4	10.8	3.3
Fe ₂ O ₃	2.1	1.5	2.0
Fe	0.8	0.7	0.6
MgO	1.9	3.8	3.0
TiO ₂	1.2	1.0	0.8
Na ₂ O	0.4	1.1	1.1
K ₂ O	<u>1.9</u>	<u>2.6</u>	<u>0.3</u>
Total	99.4	99.0	98.8
.....			
CaO/SiO ₂	0.15	0.14	0.42
Ferritic content	8	20	30

^aGiven as oxide unless otherwise indicated; carbon- and SO₃-free.

$$^b \text{Ferritic content} = \frac{\text{wt \% Fe}_2\text{O}_3}{\text{wt \% Fe}_2\text{O}_3 + 1.11 \text{ wt \% FeO} + 1.43 \text{ wt \% Fe}}$$

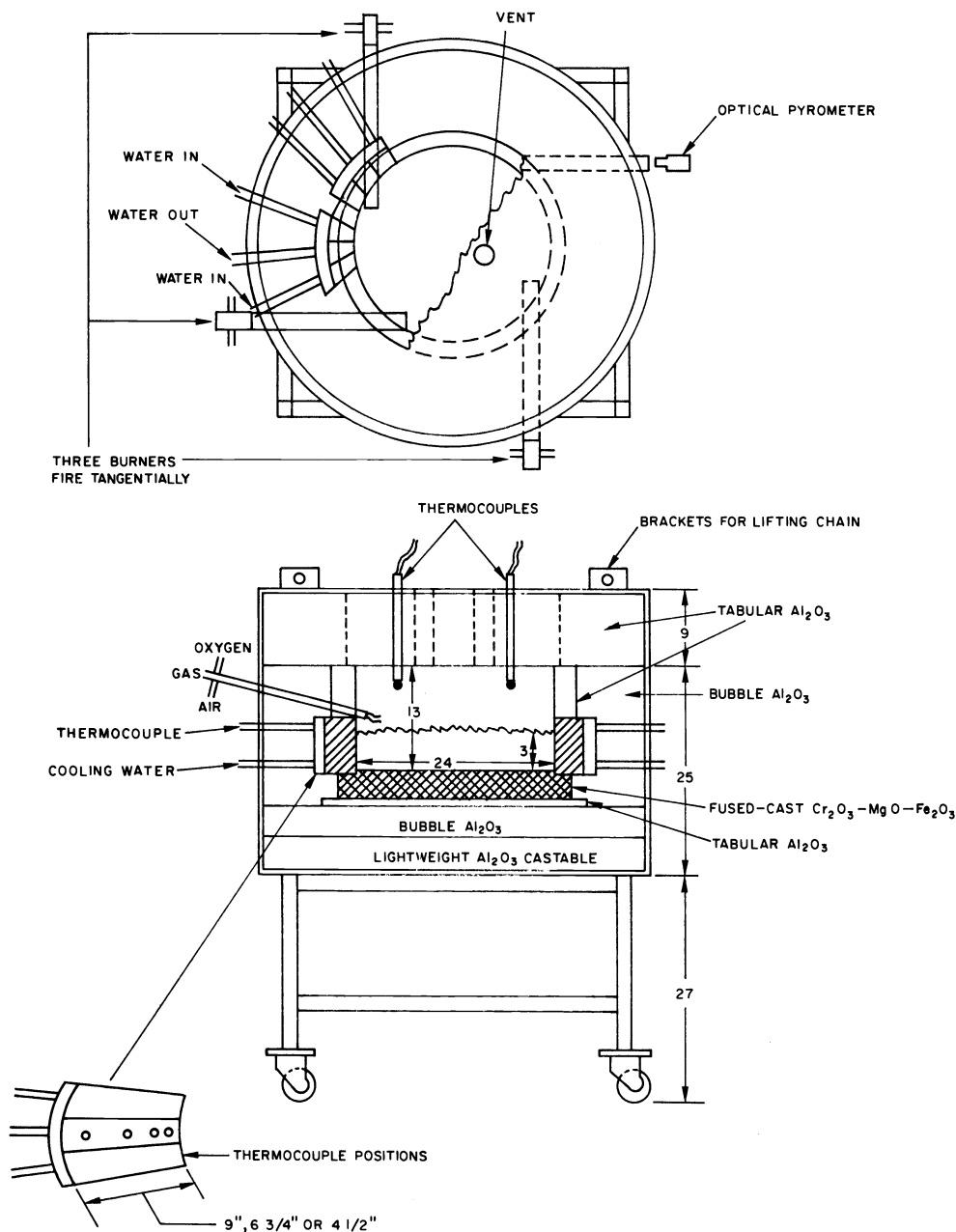


Fig. 1. Schematic of the furnace utilized to evaluate mineral-residue/refractory compatibility. All dimensions are in inches.

At the conclusion of the test, after the furnace reached room temperature and the insulating ring was removed, a visual inspection revealed that several of the refractories were cracked. The most seriously cracked refractories were the dense high-chromia products, including numbers 22, 38, 255, 280, and one brick of number 812 (see Table 1 for composition).

The bricks were then sectioned lengthwise so that the depths of removal and penetration (both from the original hot face) could be measured. Two areas of attack were visible, corresponding to the two levels of the MR pool. Since the pool is heated only from the top, a strong vertical gradient exists. Thus, most of the attack takes place at or near the surface of the bath. The addition of extra MR in the second phase of the test (at 1500°C) serves to preserve the degree of corrosion that has occurred in the first phase of the test (at 1600°C).

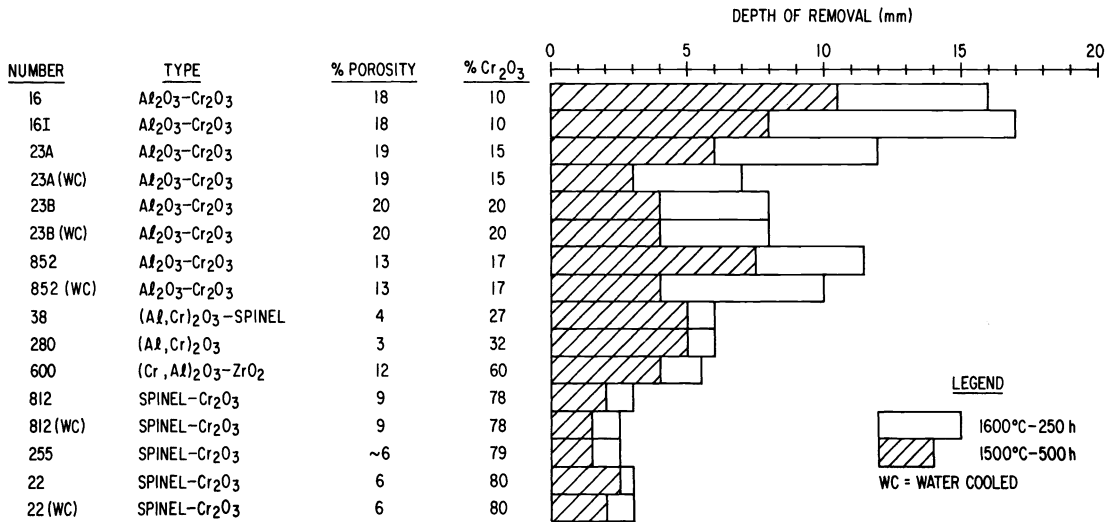


Fig. 2. Relative corrosion resistances of refractories in Test 2400B.

The relative corrosion resistances of the refractories are given in Fig. 2. Differences of <1 mm in the depth of removal may not be significant. Note that numbers 812, 22, 23A, 23B, and 852 were tested both with and without water cooling. A calcium-aluminate-bonded intermediate-alumina castable was placed between the cold ends of the refractories and the water-cooled chills in an effort to promote effective cooling.

The most corrosion-resistant refractories, at both 1500 and 1600°C, were the dense ~80% chromia refractories, i.e., numbers 255, 812, and 22. The corrosion rates (mm/h) of the uncooled bricks of these refractories were about 2.5 to 4 times faster at 1600°C than at 1500°C. Although the effect of water cooling on the 228-mm bricks of these high-chromia refractories was too small to assess accurately in this test, the corrosion rates of the alumina-chromia refractories, i.e., numbers 23A and 852, decreased significantly (by a factor of ~2 at 1500°C) when the bricks were cooled. The results of past experiments suggest that the water-cooled refractories should perform substantially better than uncooled refractories as the length of the refractory decreases.

Some differences in the ranking of the refractories at 1600 and 1500°C were observed. At 1600°C, increasing chromia content clearly resulted in increased corrosion resistance. At 1500°C, the water-cooled sintered alumina-chromia (15-20%) refractories, i.e., numbers 23A, 23B, and 852, exhibited slightly less corrosion than did the uncooled intermediate-(27-32%) chromia fused-cast refractories, i.e., numbers 38 and 280. Note that the uncooled number 23B also suffered less corrosion than the intermediate-chromia refractories. Nevertheless, the amount of MR penetration was significantly greater for the more porous sintered alumina-chromia refractories. Increasing the temperature from 1500 to 1600°C increased the corrosion rates (which were found to be independent of time) by a factor of 3-4 for the uncooled alumina-(10-20%) chromia refractories.

Test 2400A

This test evaluated the compatibility of 14 refractory bricks (~228 mm in length) with a very acidic ($\text{CaO/SiO}_2 = 0.14$) low-iron oxide MR (Table 2). The furnace was raised to 1600°C and held at that temperature for 250 h. At this point, the furnace was cooled to room temperature to allow visual inspection. Since little corrosion was evident, the test was continued at 1600°C without further additions of MR. The test was finally terminated (owing to a failure of the exhaust fan) after a total of 475 h at a plenum temperature of ~1600°C. Results of the tests have been summarized in Fig. 3. Note that bricks of numbers 812, 22, 852M, 23A, and 23B were tested both with and without water cooling. A phosphate-bonded silicon carbide mortar was utilized between the cold ends of the refractories and the water-cooled chills to promote more effective heat transfer than in test run 2400B (in which a calcium-aluminate-bonded intermediate-alumina castable was used). Owing to the high viscosity of MR 2400A, very little corrosion occurred during this test. Comparison of the corrosion data with test 2400B-1 indicates that the corrosion rates (mm/h) at 1600°C were about 4-8 times higher in MR 2400B (note that test 2400B-1 lasted only 475 h, whereas test 2400A lasted 500 h). Despite the low rate of corrosion, the results clearly indicate that the dense chrome-spinel products, i.e., numbers 812, 22, and 255, were superior to the others. Numbers 600, 280, and 38 also performed well. The rebonded fused-grain, chrome-spinel refractory (number 812) was ~3 times more resistant than either number 300 or number 412 (which contained free MgO), ~4 times better than number 23, and ~6 times better than number 16.

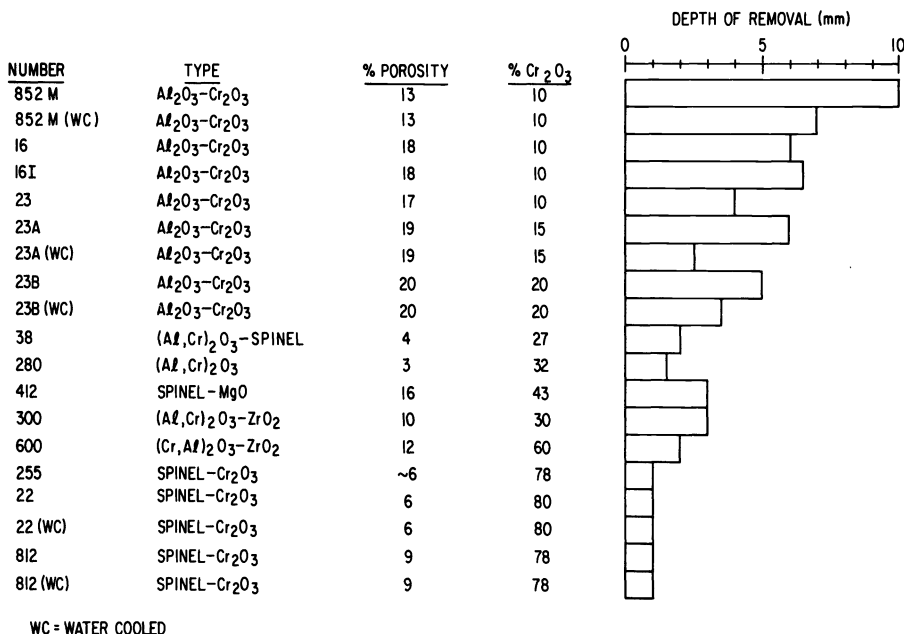


Fig. 3. Relative corrosion resistances of refractories in Test 2400A at 1600°C for 500 h.

Water-cooled alumina-chromia refractories, i.e., numbers 16, 23A, 23B, and 852M, exhibited 30-60% less corrosion than did identical uncooled refractories. Again, the magnitude of this effect can be expected to increase as the brick length decreases. However, since the chrome-spinel refractories, i.e., numbers 812 and 22, suffered only minimal corrosion, the effect of water cooling on their performance cannot be assessed accurately.

As observed upon post-test inspection, almost all of the bricks that were water cooled (with the exception of number 812) cracked during the test. In particular, the cold face of one of the bricks of number 23B crumbled into powder, indicating poor cold strength. In addition, uncooled bricks of numbers 22, 255, 38, 280, and 852M were obviously cracked.

Test 2400C

The MR in this test was a moderately acidic ($\text{CaO/SiO}_2 = 0.42$) low-iron oxide residue (Table 2). Full- (228 mm), 2/3-, and 1/2-length bricks of 11 different refractories were evaluated. The 2/3- and 1/2-length bricks were water cooled whereas the full-length bricks were not. As in test 2400A, a phosphate-bonded silicon carbide mortar was utilized between the cold ends of the refractories and the water-cooled chills to promote effective heat transfer.

This test, like test 2400B, consisted of two parts. In test 2400C-1, the furnace plenum temperature was held at 1600°C for 250 h with an MR pool 45 mm in depth (corresponding to 47 kg of MR). Then, for test 2400C-2, 33 kg of additional residue was added to bring the pool depth to 75 mm, and the furnace was held at 1500°C for a total of 500 h.

Results of the test have been summarized in Fig. 4 and again clearly indicate that the high-chromia refractories, i.e., numbers 812, 22, 255, 800, and 251A, are superior to the high-alumina refractories, i.e., numbers 23, 100, 16, and 23B. The effect of temperature on the corrosion rates is again pronounced. For the high-alumina products (full-length bricks), the corrosion rates (mm/h) at 1600°C are about 4-6 times higher than at 1500°C. For the 1/2-length high-alumina bricks, the rates are about 7-13 times higher at 1600°C than at 1500°C. Although accurate assessment of the ratios of the corrosion rates at 1600 and 1500°C for the high-chromia bricks is impossible because of the minimal corrosion at the lower temperature, the data indicate that this ratio for the full-length high-chromia refractories falls between 6 and 14.

The strong temperature dependence of the corrosion rates of the high-alumina refractories is reflected in the significantly lower corrosion rates of the water-cooled 2/3- and 1/2-length bricks when compared to the uncooled full-length bricks. In general, the 1/2-length high-alumina bricks suffered only half as much corrosion as the full-length bricks. The observed effect of water cooling is not as pronounced for the high-chromia refractories, owing to the uncertainty in measuring such small amounts of corrosion. Nevertheless, the data at 1600°C for numbers 251B, 251A, and 255 indicate ~40-50% lower corrosion rates for 1/2-length bricks.

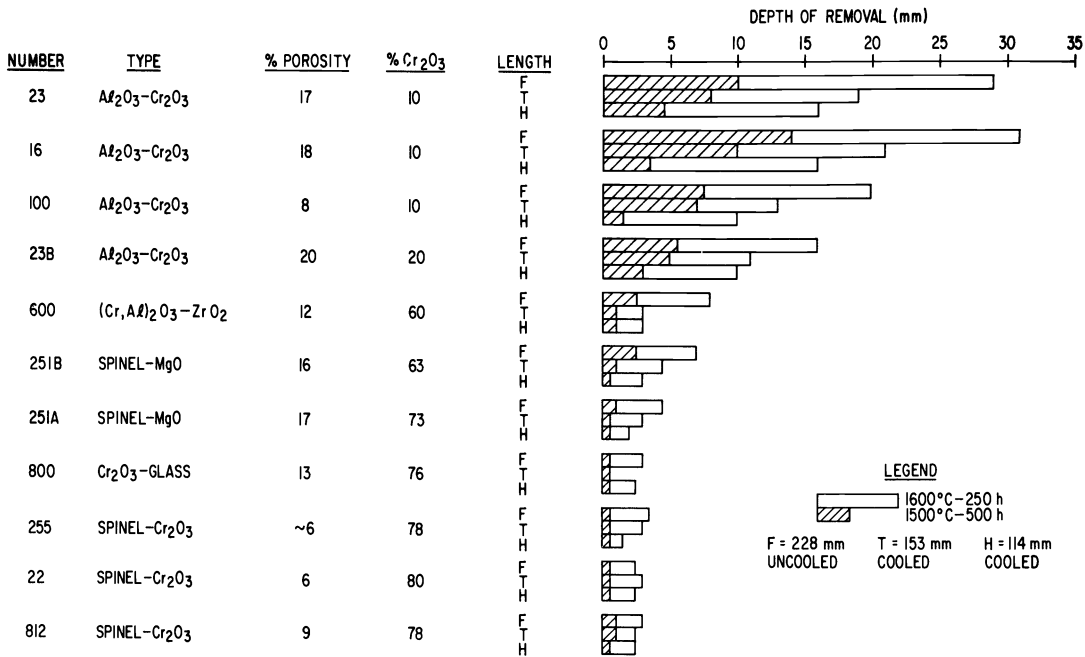


Fig. 4. Relative corrosion resistances of refractories in Test 2400C.

As in previous tests, several of the bricks had obvious fractures prior to their removal from the furnace. In particular, bricks of numbers 255, 100, and 23B were fractured. As in test 2400A, one brick (2/3 length) of number 23B crumbled into a pile of powder at the cold face.

CORROSION MECHANISMS

Number 255

As-received. This pressed and sintered refractory was composed mainly of fine (~10-20 μ m) chromia (Cr₂O₃) and chrome-rich spinel [(Mg,Fe)(Cr,Al)₂O₄] grains, primarily bonded with a silica- and titania-rich glassy phase. Some direct bonding was also evident. Pores (2-10%) were small (~10 μ m) and not interconnected.

Exposed to MR 2400B at 1600°C. As seen in Figs. 5 and 6, Fe⁺² and Al⁺³ from the MR has penetrated and reacted with the refractory to form a 50- μ m-thick (Fe,Mg)(Al,Cr)₂O₄ spinel layer at the MR-refractory interface. The Cr₂O₃ grains near the interface have been converted into this spinel, whereas the original spinel has been altered in composition by the substitution of Fe⁺² for Mg⁺² and Al⁺³ for Cr⁺³. Fe⁺² was observed to penetrate much more deeply than Al⁺³. The refractory slowly dissolved by this process. Intergranular attack was minimal.

Exposed to MR 2400B at 1500°C. Same as above, but the spinel layer was only 10 μ m thick and more intergranular attack was observed.

Number 22

As-received. This fused-cast refractory consisted primarily of a sesquioxide solid solution (Cr,Al)₂O₃ within a complex chrome-rich spinel (Mg,Fe)(Cr,Al)₂O₄ matrix. Some siliceous glass was also present.

Exposed to MR 2400B at 1600°C with Water Cooling. The mechanism of degradation again was the replacement of Mg⁺² and Cr⁺³ in the original spinel by Fe⁺² and Al⁺³. This resulted in a low-melting spinel which dissolved slowly. Very little intergranular corrosion was observed.

Exposed to MR 2400B at 1500°C. The corrosion mechanism was identical with that described above, except that the altered spinel layer was significantly thinner.

Number 812

As-received. This consisted primarily of rebonded fused-cast chrome-rich spinel (MgCr₂O₄) grain with excess chromia (Cr₂O₃). The range of grain sizes was very large (<5 to >500 μ m). The pores were irregular in shape and were interconnected to a large degree.

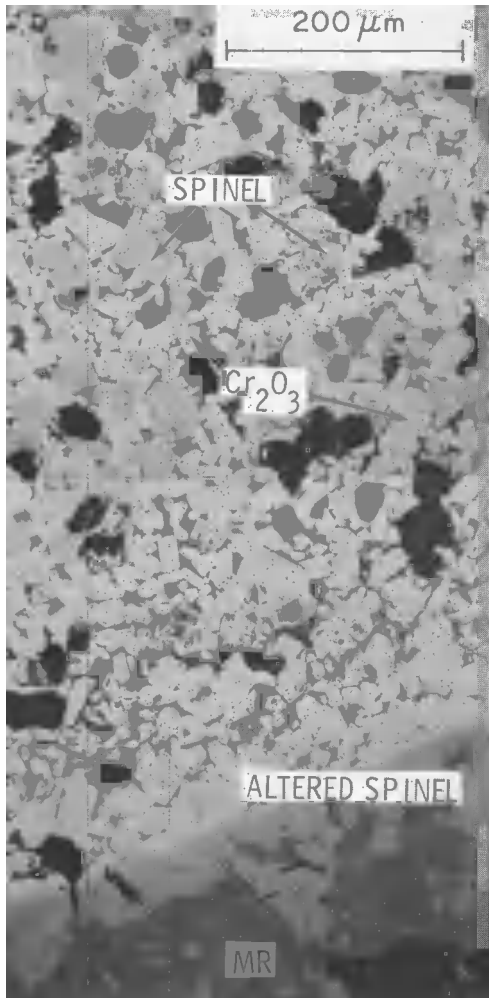


Fig. 5. Optical micrograph of Number 255 after exposure to MR 2400B at 1600°C .

Note: Fig. 6 is printed on the following page

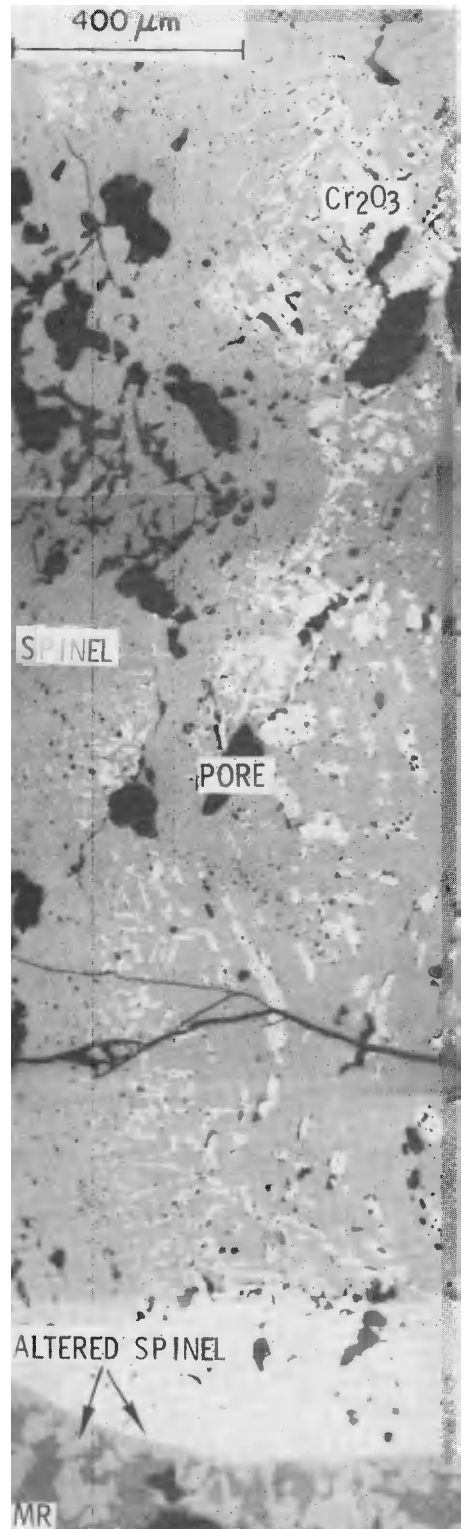


Fig. 7. Number 812 after exposure to MR 2400B at 1600°C .

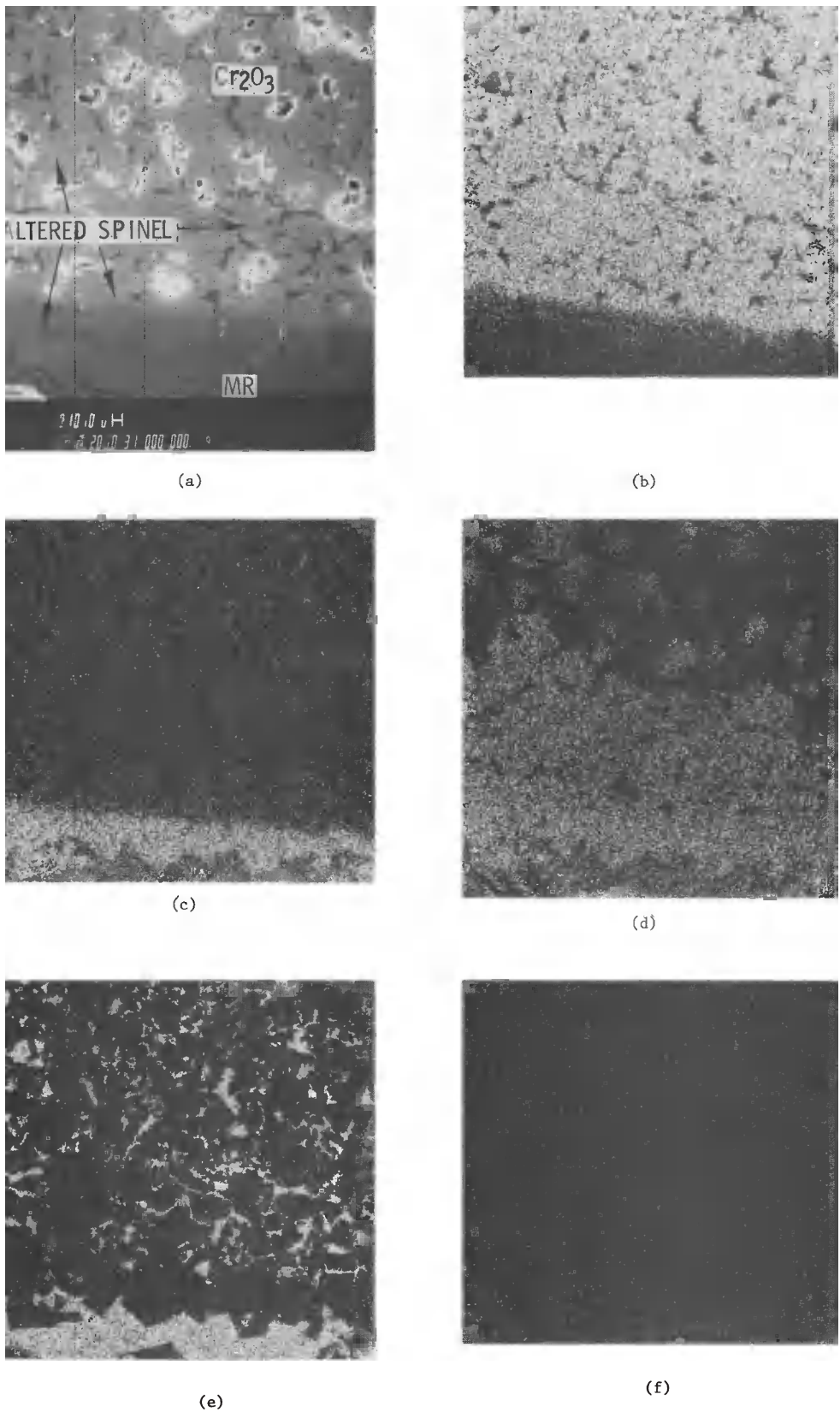


Fig. 6. Number 255 after exposure to MR 2400B at 1600°C. (a) Scanning electron micrograph; elemental scans for (b) Cr, (c) Al, (d) Fe, (e) Si, and (f) Mg.

Exposed to MR 2400B at 1600°C. The corrosion mechanism of the grain was identical with that observed in refractories number 22 and 255. However, the refractory was highly penetrated by the MR through the irregular porosity (Fig. 7). Note that the spinel and chromia phases appeared to be attacked at similar rates. Examination of a core taken 25 mm from the hot face revealed that the MR had penetrated to this depth. Intergranular corrosion was evident.

Exposed to MR 2400B at 1500°C. The attack was similar to that observed at 1600°C, except that the altered spinel was somewhat thinner.

Number 600

As-received. This refractory was composed primarily of grains of chromia-alumina sesquioxide solid solution $[(\text{Cr},\text{Al})_2\text{O}_3]$, with some zirconia (ZrO_2) also present. Extensive siliceous bonding was evident. X-ray analysis failed to indicate the presence of ZrSiO_4 .

Exposed to MR 2400B at 1600°C. ZrO_2 has been preferentially dissolved (Fig. 8). The $(\text{Cr},\text{Al})_2\text{O}_3$ grains have reacted with the FeO from the MR to form a loose network of $\text{Fe}(\text{Cr},\text{Al})_2\text{O}_4$ spinel which can be seen floating in the Si^{+4} -rich MR. This spinel dissolved much more slowly than did the ZrO_2 . As indicated by the Fe and Si scans, the MR has penetrated into the siliceous bonding phase an additional 400-500 μm past the remaining ZrO_2 .

Number 16

As-received. This refractory was composed of alumina (Al_2O_3) grains with an alumina-chromia $[(\text{Al},\text{Cr})_2\text{O}_3]$ solid-solution bond. No glassy phase was present.

Exposed to MR 2400B at 1600°C. Note the formation of a thin spinel layer (FeAl_2O_4) at the MR-refractory interface (Fig. 9), as well as spinel crystallites at the grain boundaries. Extensive intergranular attack was also evident.

Exposed to MR 2400B at 1500°C. The attack was similar to that observed at 1600°C except that the spinel layer was thinner. Precipitation of spinel crystals in the MR was also evident.

Exposed to MR 2400A at 1600°C. Extensive intergranular attack was evident (Fig. 10). Note that the alumina grains can be seen floating away in the MR. No intermediate reaction products, such as spinels, were observed to form.

Number 23B

As-received - This refractory consisted of alumina grains with an alumina-chromia solid-solution bond. No glassy phase was present.

Exposed to MR 2400A at 1600°C. Extensive intergranular attack was evident (Fig. 11). A loose network of spinel reaction product can be seen floating in the MR at the interface.

Number 800

As-received. This refractory was composed of chromia (Cr_2O_3) grains in a siliceous glass matrix.

Exposed to MR 2400C at 1600°C. The chromia grains have reacted with Fe^{+2} and Al^{+3} in the MR to produce an $\text{Fe}(\text{Cr},\text{Al})_2\text{O}_4$ spinel which can be seen floating in the MR (Fig. 12).

Number 251A

As-received. This refractory was composed of rebonded fused-cast chrome-rich spinel (MgCr_2O_4) grains with some excess MgO present. The structure was highly porous.

Exposed to MR 2400C at 1600°C. Spinel grains dissolved slowly as Fe^{+2} and Al^{+3} from the MR exchanged with Mg^{+2} and Cr^{+3} ; the free MgO was preferentially dissolved. The MR penetrated into the structure easily, with resultant intergranular attack.

DISCUSSION

The corrosion data from these tests can only be used to provide a semiquantitative, relative ranking of the performance of the refractories. The data cannot be used directly to predict lining lifetimes in an actual application, since the velocity of the MR may be significantly different. Of the three major mechanisms of the corrosion process, i.e., dissolution, penetration/disruption, and erosion, the present tests tend to emphasize the first two owing to the low velocity of the MR at the interface with the refractory. In applications with higher-velocity MR, the rate of corrosion can be anticipated to increase significantly owing to increased rates of dissolution and/or erosion. This could be particularly pronounced for those refractories that exhibited substantial intergranular attack, which might lead to the erosion of entire grains.

The importance of high chromia content and density in minimizing the attack is evident from these data. Although substantial differences exist in the structures and bonding of the most corrosion-resistant refractories, i.e., numbers 812, 22, 255, 800, and 251A, the data from these tests fail to indicate any significant differences in the corrosion rates of these refractories. Further tests in an environment with a higher-velocity MR are necessary.

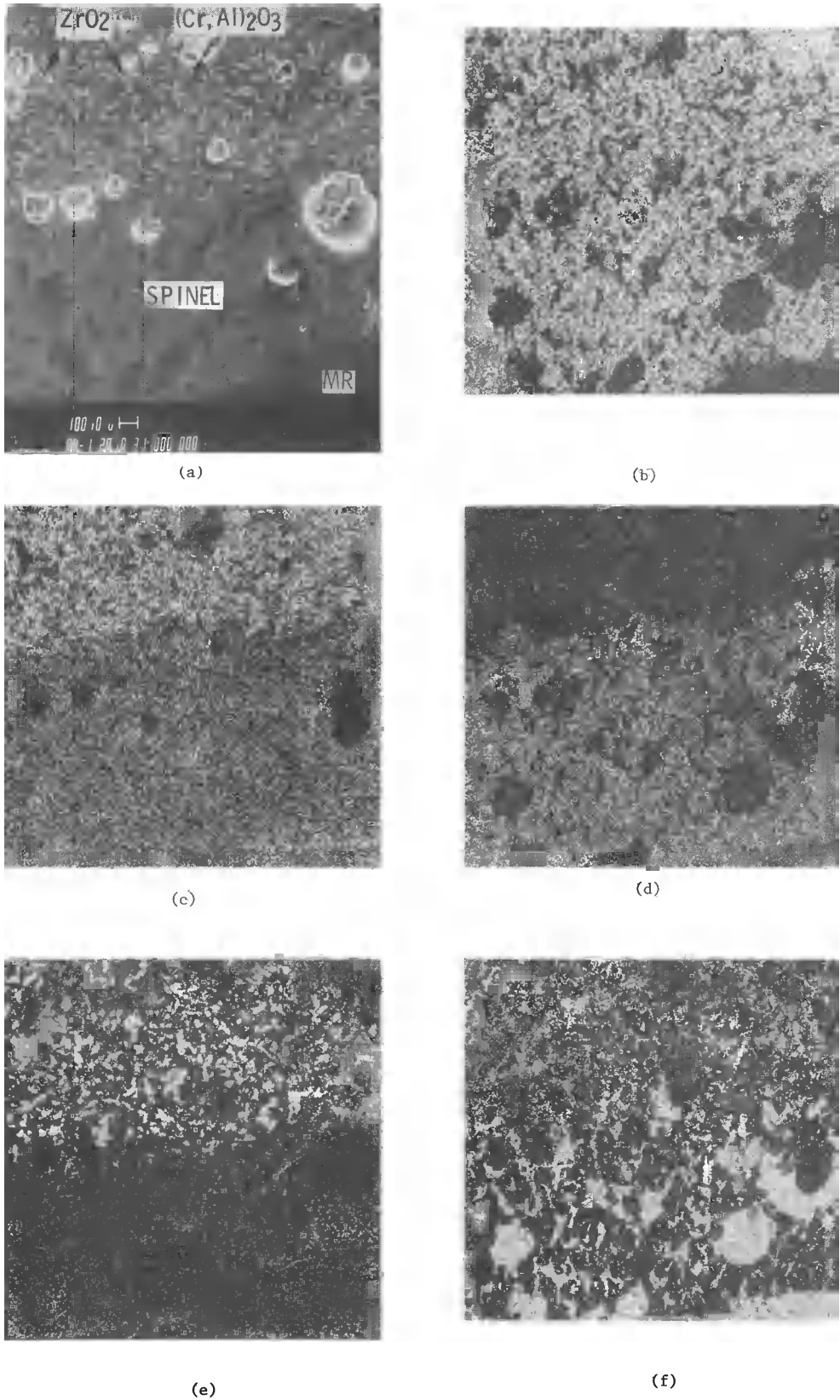


Fig. 8. Number 600 after exposure to MR 2400B at 1600°C. (a) Scanning electron micrograph; elemental scans for (b) Cr, (c) Al, (d) Fe, (e) Zr, and (f) Si.

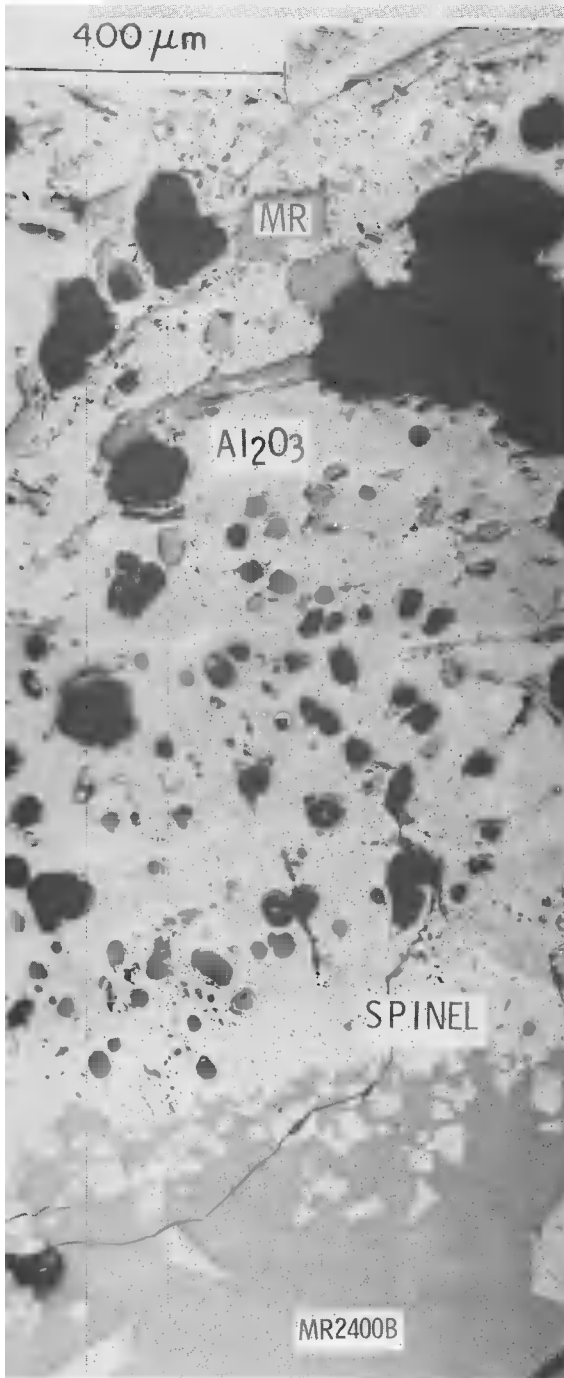


Fig. 9. Number 16 after exposure to MR 2400B at 1600°C .

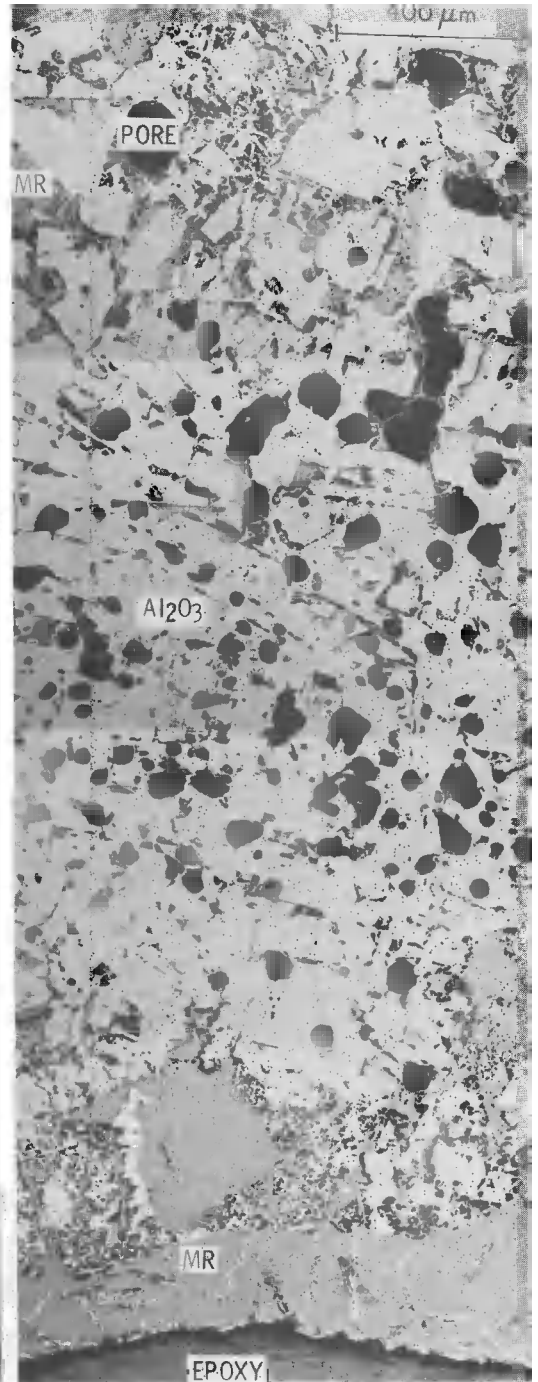


Fig. 10. Number 16 after exposure to MR 2400A at 1600°C .

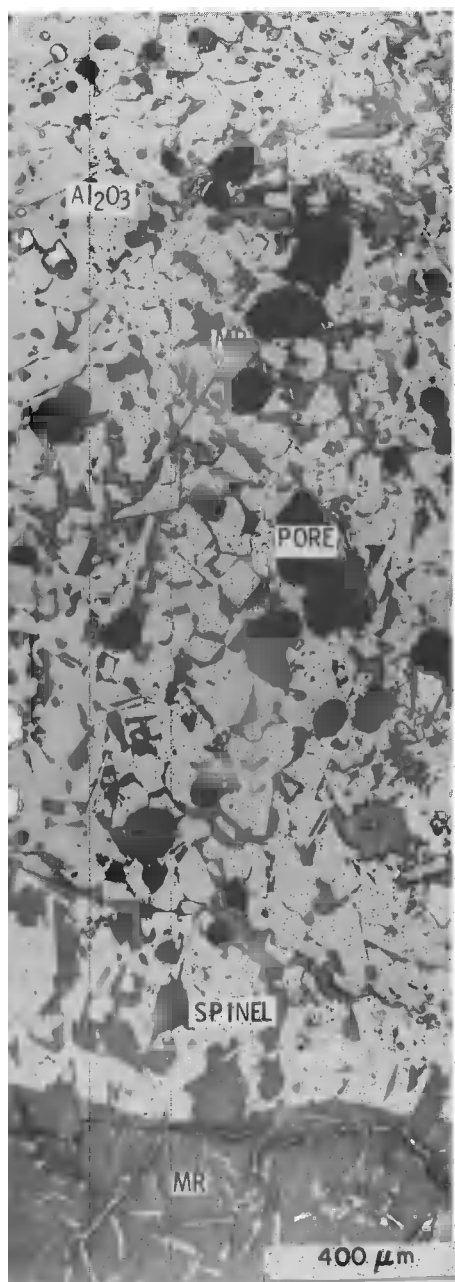


Fig. 11. Number 23B after exposure to MR 2400A at 1600°C.

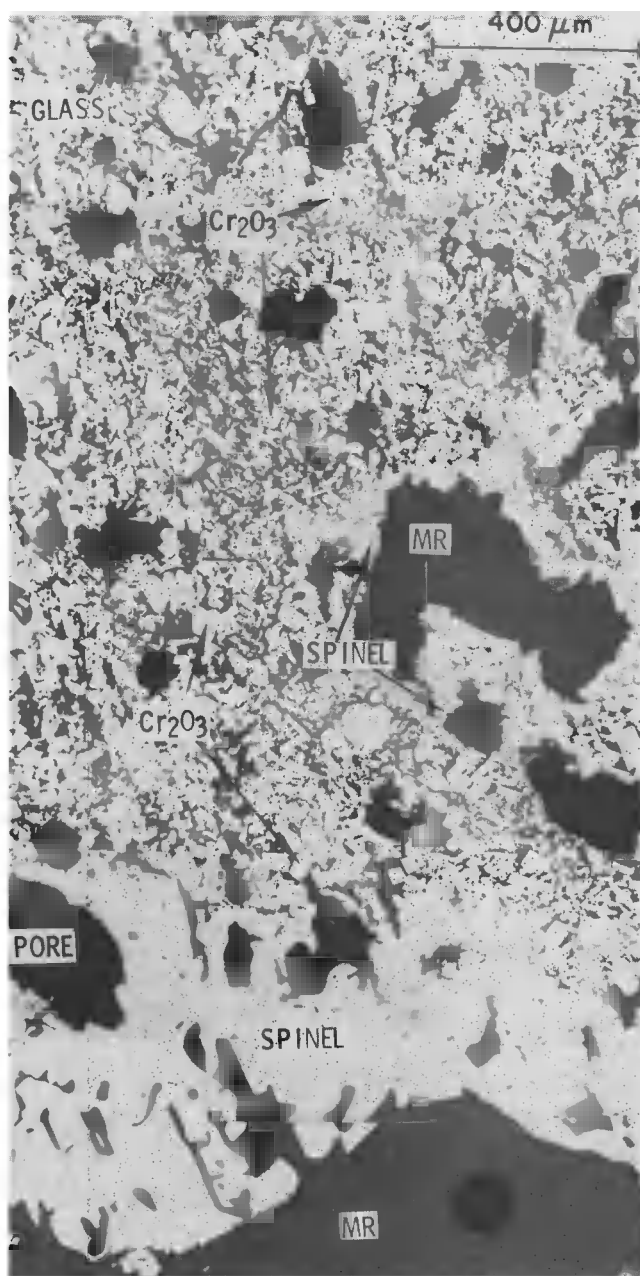


Fig. 12. Number 800 after exposure to MR 2400C at 1600°C.

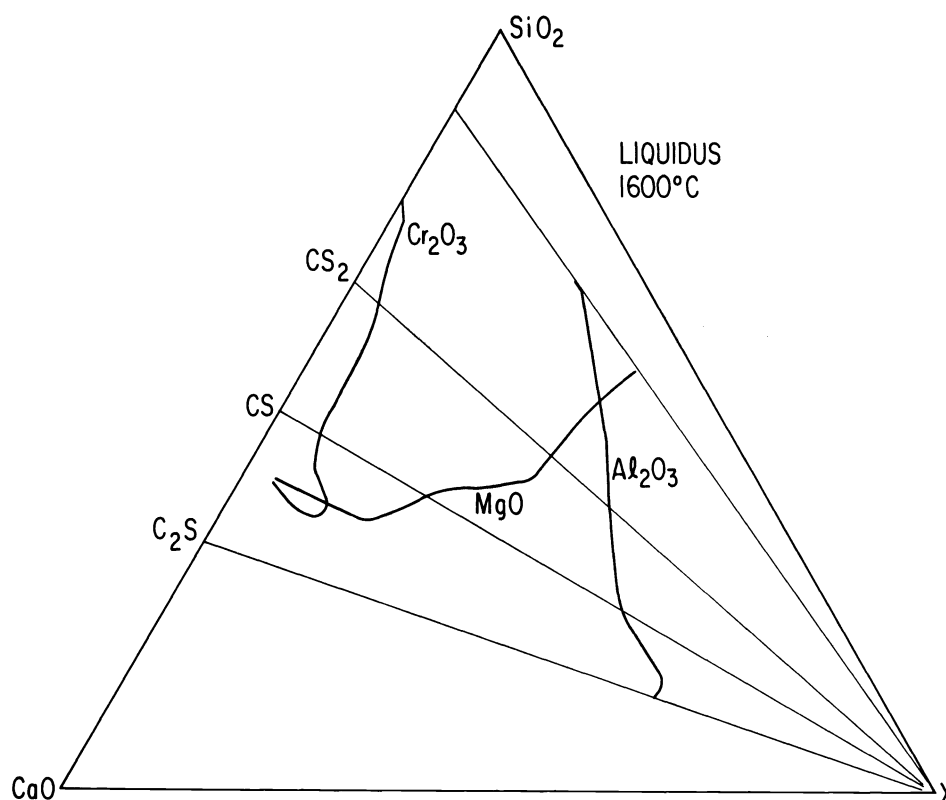


Fig. 13. Liquidus compositions (wt %) at 1600°C in the $\text{SiO}_2\text{-CaO-X}$ ternary system, where $X = \text{Cr}_2\text{O}_3, \text{Al}_2\text{O}_3, \text{or MgO}$.

The superior corrosion resistance of chromia-based refractories may possibly be attributed to a number of factors. At present, the exact effects of the spinel reaction layers on the kinetics of dissolution are unknown. Certainly if the spinel reaction layer is dense and adherent, the surface area of a porous refractory exposed to the MR will be reduced and attack will be retarded. Previous results (Ref. 1) have also indicated that Cr^{+3} -rich spinels are more resistant to fluxing by $\text{FeO-SiO}_2\text{-CaO}$ liquids than are Al^{+3} -rich spinels. According to the work of Cooper and King (Ref. 2), the rate of dissolution of oxides in CaO-SiO_2 liquids is generally controlled by diffusion through a boundary layer in the MR that is adjacent to the refractory. The rate at which refractories are attacked in MRs can be expressed by

$$j = \frac{D(C_1 - C_\infty)}{\delta(1 - C_1 \bar{V})}, \quad (1)$$

where j = number of moles removed per second per square centimeter,
 D = effective diffusion coefficient through the boundary layer,
 C_1 = concentration of the solute at the interface,
 C_∞ = concentration of the solute in the bulk liquid,
 δ = thickness of the boundary layer, and
 \bar{V} = partial molar volume;

therefore, the solubility limits of the candidate materials in siliceous liquids are important parameters.

As can be deduced from the pertinent phase diagrams, the amount of Cr_2O_3 that is soluble (in an oxidizing atmosphere) in a liquid with $\text{CaO/SiO}_2 < 1$ at 1600°C is substantially smaller than the amounts of either MgO or Al_2O_3 (Fig. 13). Even though the mineral residues in these experiments contain substantial amounts of Al_2O_3 (14-26 wt %), some MgO (1-4%), and little or no Cr_2O_3 , the quantity $(C_1 - C_\infty)$ is almost always smallest (i.e., the driving force for dissolution lowest) for Cr_2O_3 . Unfortunately, little information is currently available on the diffusion coefficients of the various species of interest in siliceous melts, or on the thickness of the boundary layer, so that accurate predictions of the flux from Eq. (1) are not possible. However, it is possible to infer that as the CaO/SiO_2 ratio increases and as

the Al_2O_3 content of the MR decreases, the ratio of the corrosion rates of Al_2O_3 - to Cr_2O_3 -based refractories should increase. As shown in Table 3, the ratios of the corrosion rates for number 16/number 812 at 1600°C are similar in MR 2400B and MR 2400A (both of which have $\text{CaO/SiO}_2 \sim 0.15$ and $\text{Al}_2\text{O}_3 \sim 23\%$). However, in MR 2400C (which has $\text{CaO/SiO}_2 = 0.42$ and only 14.6% Al_2O_3), the ratio increases, as would be expected, to 10.3.

TABLE 3. Ratio of the depths of removal at 1600°C for refractory number 16/refractory number 812 as a function of composition of the mineral residue

	MR 2400B	MR 2400A	MR 2400C
Depth of removal (number 16/number 812)	5.3	6.0	10.3
CaO/SiO_2	0.15	0.14	0.42
Al_2O_3 (wt %)	22.8	23.6	14.6

Although dense high-chromia refractories have demonstrated superior corrosion resistances, they are sensitive to thermal shock. This is particularly true for the fused-cast refractories, i.e., numbers 22, 38, and 280, and also for number 255. Water cooling tends to aggravate this problem.

Although not observed in these tests, iron oxide bursting (Ref. 3) is a potential problem. Refractories composed of either pure Cr_2O_3 or MgCr_2O_4 will react with iron oxide to form FeCr_2O_4 spinel. In the case of Cr_2O_3 refractories, the change in structure associated with this reaction may be sufficient to cause spalling or bursting, particularly if the refractory has been significantly penetrated by the MR. In the case of MgCr_2O_4 refractories, iron oxide bursting may only occur as a result of alternate oxidizing and reducing cycles which cause $\text{Fe}^{+2}\text{Cr}_2\text{O}_4$ to decompose to an $(\text{Fe}^{+3}, \text{Cr})_2\text{O}_3$ solid solution, with a devastating volume change. The severity of this problem can be minimized by (1) utilizing dense materials that limit the reaction to the surface of the refractory; (2) introducing bonding phases, such as SiO_2 , which inhibit penetration of the MR into the refractory by increasing the viscosity; or (3) controlling the iron oxide content of the MR.

CONCLUSIONS

The compatibility of a variety of refractories with three different siliceous mineral residues at temperatures between 1500 and 1600°C in a low-oxygen atmosphere has been investigated. Dense high-chromia (~80 wt %) refractories, i.e., numbers 812, 22, 255, 251A, and 800, have demonstrated superior resistance to corrosion but appear to be sensitive to thermal-shock damage. The superiority of the chromia-based refractories to the alumina-based refractories increased as the CaO/SiO_2 ratio increased and as the Al_2O_3 content of the MR decreased. Water cooling significantly reduced the corrosion of many of the refractories tested but aggravated the thermal-shock damage problem.

Acknowledgments - The author gratefully acknowledges the experimental assistance of F. L. Morris, P. M. Chapello, and R. J. Fousek.

REFERENCES

1. C. R. Kennedy, submitted to the J. Mater. Energy Syst. (June 1981).
2. A. R. Cooper, Jr. and W. D. Kingery, J. Amer. Ceram. Soc. 47, 37-43 (1964).
3. J. H. Chesters, Refractories: Production and Properties, pp. 213-261, The Iron and Steel Institute, London (1973).